ACS APPLIED MATERIALS & INTERFACES

www.acsami.org

Research Article

Responsive Hydrogel Binding Matrix for Dual Signal Amplification in Fluorescence Affinity Biosensors and Peptide Microarrays

Simone Hageneder, Vanessa Jungbluth, Regina Soldo, Christian Petri, Matthias Pertiller, Marjut Kreivi, Andreas Weinhäusel, Ulrich Jonas, and Jakub Dostalek*

Cite This: *ACS Appl. Mater. Interfaces* 2021, 13, 27645−27655

Read Online

ACCESS | Metrics & More | Article Recommendations | Supporting Information

ABSTRACT: A combined approach to signal enhancement in fluorescence affinity biosensors and assays is reported. It is based on the compaction of specifically captured target molecules at the sensor surface followed by optical probing with a tightly confined surface plasmon (SP) field. This concept is utilized by using a thermoresponsive hydrogel (HG) binding matrix that is prepared from a terpolymer derived from poly(*N*-isopropylacrylamide) (pNIPAAm) and attached to a metallic sensor surface. Epi-illumination fluorescence and SP-enhanced total internal reflection fluorescence readouts of affinity binding events are performed to spatially interrogate the fluorescent signal in the direction parallel and perpendicular to the sensor surface. The pNIPAAm-based HG binding matrix is arranged in arrays of sensing spots and employed for the specific detection of human IgG antibodies against the Epstein−Barr virus (EBV). The detection is performed in diluted human plasma or with isolated human IgG by using a set of peptide ligands mapping the epitope of the EBV nuclear antigen. Alkyne-terminated peptides were covalently coupled to the pNIPAAm-based HG carrying azide moieties. Importantly, using such low-molecular-weight ligands allowed preserving the thermoresponsive properties of the pNIPAAm-based architecture, which was not possible for amine coupling of regular antibodies that have a higher molecular weight.

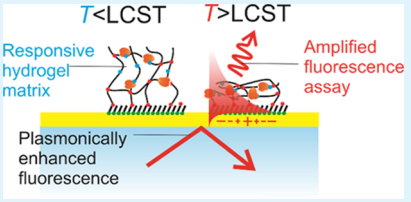

KEYWORDS: *thermoresponsive hydrogel, pNIPAAm, plasmon-enhanced fluorescence, microarrays, click chemistry, peptide, serotesting, biomarkers*

INTRODUCTION

Responsive hydrogel (HG) materials are increasingly employed in optical analytical technologies, where they are employed to serve in three-dimensional binding matrices for the specific capture of the target analyte and to suppress unspecific interactions of abundant molecules present in the analyzed liquid samples,[1,2] facilitate readout and amplify the sensor response to specific binding events,[3] and allow for manipulating small volumes of analyzed aqueous samples on miniature sensor chips.[4]

Responsive HGs are often combined with metallic nanostructures, and among others, their on-demand swelling and collapse were utilized in colorimetric[5] and surface-enhanced Raman spectroscopy (SERS)-based sensors.[6−8] These sensor modalities take advantage of the resonant excitation of surface plasmons (SPs) that exhibit a tightly confined profile of the electromagnetic field associated with collective oscillations of the charge density at the metal surface. The implementation of responsive HGs allows for the active control of near-field coupling between localized SPs at metallic nanoparticles,[9] and they can be tailored to trap target molecules and deliver them to the zones referred to as plasmonic hotspots. The plasmonic confinement of electromagnetic field intensity at such hotspots was further enhanced by approaching metallic nanostructures through the collapse of a responsive HG that serves as a host material or a thin spacer.[6,10]

The majority of thermoresponsive HGs used in the analytical technologies are derived from poly(*N*-isopropylacrylamide) (pNIPAAm), a polymer exhibiting a lower critical solution temperature (LCST) of 32 °C,[11] at which it switches between a hydrophilic expanded state (T < LCST) and a hydrophobic collapsed state (T > LCST). In order to allow for post-modification of the pNIPAAm network with functional biomolecules, mostly copolymers have been used for the incorporation of moieties enabling the controlled coupling of protein molecules.[12,13] The large surface area of HG films renders them the ability to host high amounts of biomolecules that can function as ligands in affinity biosensors. Such an extended three-dimensional biointerface can affinity-bind target molecules from the analyzed samples with an efficiency that outperforms that of traditionally used two-dimensional surface architectures in surface plasmon resonance (SPR) and

Received: March 31, 2021
Accepted: April 28, 2021
Published: June 3, 2021

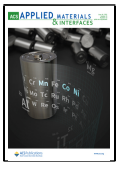

Downloaded via 62.218.164.126 on June 28, 2021 at 15:11:45 (UTC).
See https://pubs.acs.org/sharingguidelines for options on how to legitimately share published articles.

© 2021 The Authors. Published by American Chemical Society

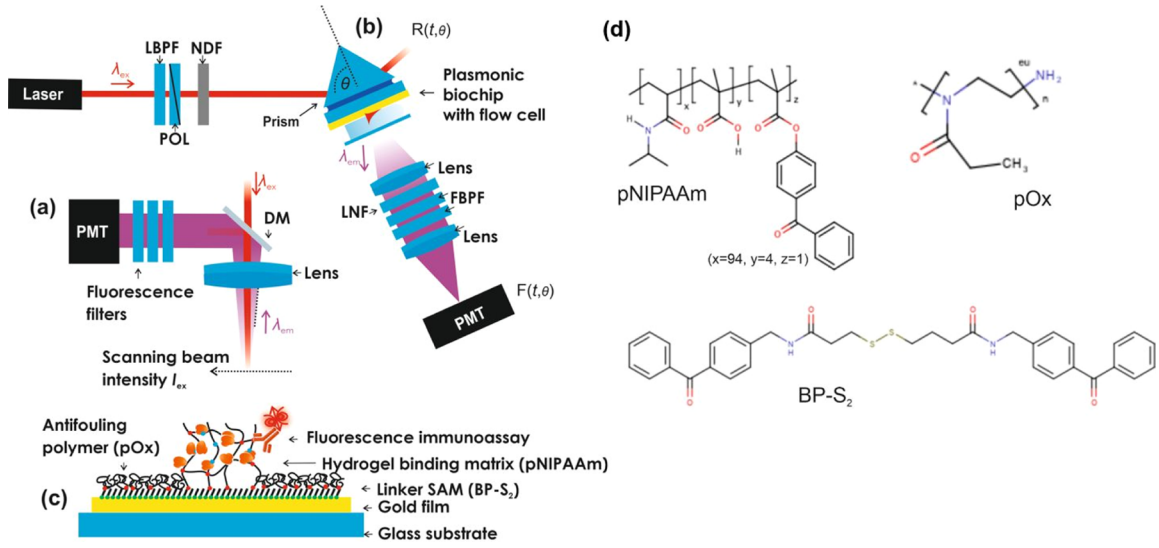

Figure 1. Optical configuration used for the readout of affinity binding on the biochip with arrays of HG sensing spots based on (a) epi-illumination fluorescence configuration (EPF) and (b) total interal reflection fluorescence (TIRF) readout combined with SPR that utilizes a laser band pass filter (LBPF), polarizer (POL), neutral density filter, laser notch filter (LNF), fluorescence bandpass filter (FBPF), and photomultiplier (PMT). (c) Schematics of the biochip with arrays of HG sensing spots and (d) chemical structure of the used photocross-linkable pNIPAAm-based polymer, passivating polyoxazoline (pOx), and the benzophenone-disulfide ($BP-S_2$) linker forming a SAM on the gold surface of the biochip.

surface plasmon-enhanced fluorescence (PEF) biosensors.[12,14,15]

Similar to SERS, an improved readout accuracy can also be achieved for other types of plasmon sensors with the HG binding matrix. Then, its switching to the collapsed state can cause compaction of the specifically bound analyte to a smaller volume. This approach can be particularly beneficial for the PEF readout, as the plasmonic amplification of fluorescence emission is strongly dependent on the distance from the metal surface and requires delicate control of the biointerface architecture. However, we witnessed that only a few works have explored this concept until now. It was reported that responsive HG binding matrix-enhanced fluorescent signal amplification was carried out for PEF immunoassays with the collapse of the system triggered by ionic strength[16] and temperature[10,17] stimulus. However, these works demonstrated possible detection only in model samples, under conditions that are not suitable for practical applications, and reveal that the responsive characteristics of the used pNIPAAm-based HG matrix substantially deteriorate after conjugation with high-molecular-weight ligands such as antibodies.[10,17]

More recently, peptides have been frequently explored as ligands, offering the advantage of cost-efficient and reproducible synthesis, increased long-term stability, and more controlled ways for their immobilization.[18,19] In this work, we explore several routes to utilize a spatially resolved fluorescence readout of assays that takes advantage of arrays of antibody and peptide ligands incorporated in the pNIPAAm-based HG matrix. The possibility of using the temperature-induced collapse of the HG for compacting the captured analytes is demonstrated for the PEF readout, yielding a dual amplification functionality. This study reveals the importance of the choice of the ligand used for the post-modification of the HG matrix as only the use of low-molecular-weight components such as peptides allowed preserving the responsive properties and implementing the dual amplification concept.

EXPERIMENTAL SECTION

Materials. All reagents were used as received. 1-Ethyl-3-(3-dimethylaminopropyl)carbodiimide (EDC) was obtained from Sigma-Aldrich (Germany). Alkyne-modified peptides were custom-made by JPT (Berlin, Germany) mapping epitopes of Epstein−Barr virus (EBV) nuclear antigen or of the enzyme carbonic anhydrase XII (CA12), which can be found in literature.[20] The recognition sequences of these peptides were CA12: HLQHVKYKGQEAFVP; EBV1: PGRRPFFHPVGEADY; EBV2: AQPAPQAPYQGYQEP; EBV3: YQEPPPPQAPYQGYQ; and EBV4: FHPVGEADYFEYHQE.

The monoclonal antibody against human CA12 peptide (AMAb90639) was purchased from Atlas Antibodies, Bromma, Sweden. Goat detection antibodies anti-mouse and anti-human IgG (H + L) conjugated with Alexa Fluor 647 (anti-mIgG-AF647 and anti-hIgG-AF647) were purchased from Thermo Fisher. IgG from the mouse serum (mIgG) and human serum (hIgG), phosphate-buffered saline (PBS), Tween 20, Hellmanex III, and bovine serum albumin (BSA) were purchased from Merck-Sigma-Aldrich (Austria). Pooled human plasma samples were obtained from Innovative Research (USA). Sodium acetate buffer (ACT) was made using sodium acetate and acetic acid; both obtained from VWR Chemicals (Austria). All buffers were prepared with deionized water (Arium Pro, Sartorius Stedim). 2D-Azide Glass slides (#10400621) were purchased from PolyAn, Berlin, Germany.

Synthesis of the Polymer and Linker. 2-Azidoethan-1-aminium chloride was synthesized as follows based on the procedure in the literature:[21] 9.83 g of 2-bromoethylamine hydrobromide (48 mmol) was dissolved in 25 mL of water, to which a solution of 9.75 g of sodium azide (150 mmol) in 25 mL of water was added at room temperature. The mixture was heated at 80 °C overnight until the completion of the reaction, then the volume was concentrated to around 10 mL, and the mixture was cooled in an ice bath. The reaction conversion was followed by silica gel thin-layer chromatography (eluent: chloroform/methanol/conc. aqueous ammonia—13/5/1; staining: ninhydrine). 150 mL of diethylether was added to the flask, followed by 8 g of KOH powder under vigorous stirring and keeping the temperature below 10 °C. The organic phase was separated, and the aqueous phase was further extracted two times, with 50 mL of diethyl ether. The combined organic phases were dried over anhydrous K_2CO_3, the solvent removed, resulting in yellowish oil. Afterward, 50 mL of 4 M HCl was added. The solvent was

https://doi.org/10.1021/acsami.1c05950
ACS Appl. Mater. Interfaces 2021, 13, 27645−27655

removed and dried in a vacuum at 50 °C overnight. Yield: 4.80 g (39.2 mmol, 82%).

4-Sulfotetrafluorophenol (TFPS) and the benzophenone-disulfide BP-S2 (see Figure 1) were synthesized as described in the literature (see ref[22,23]). The pNIPAAm-based terpolymer was synthesized using *N*-isopropylacrylamide, methacrylic acid, and *N*-(4-benzoylphenyl)-acrylamide (94:5:1 ratio).[24] Shortly, 4-aminobenzophenone (20.3 mmol, 4.00 g) was dissolved in dichloromethane (DCM) (50 mL), and the solution cooled with an ice-water bath to 0 °C. Na_2CO_3 (20.3 mmol, 2.15 g) was added, and the resulting dispersion stirred for 20 min at 0 °C. Acryloyl chloride (26.4 mmol, 2.39 g, 2.12 mL) was diluted with DCM (50 mL) and added dropwise to the dispersion at 0 °C. After complete addition, the reaction mixture was allowed to warm to room temperature and stirred for 16 h. The formed solid was filtered off, and the reaction mixture extracted with aq. $NaHCO_3$ solution (5 wt %, 3 × 100 mL) and water (3 × 100 mL). The organic layer was separated and dried over $MgSO_4$, filtered, and the solvent evaporated, giving the title compound as a brownish solid. Yield: 33% (6.73 mmol, 1.69 g). ^{1}H NMR (400 MHz, chloroform-*d*): δ [ppm] = 7.85−7.46 (m, 9H); 6.51−6.47 (dd, 1H); 6.31−6.24 (dd, 1H); 5.85−5.83 (dd, 1H). Anti-fouling polymer poly(2-ethyl-2-oxazoline) (pOx) was synthesized as reported.[25]

Preparation and Structuring of HG Layers. The HG structures were prepared on BK7 or LASFN9 glass substrates, cleaned for 15 min by consecutive sonicating in 1% (v/v) Hellmanex III aqueous solution and deionized water, and a final sonication in ethanol puriss. After drying the substrates under a stream of compressed air, they were coated with 2 nm chromium and 50 nm gold by a vacuum thermal evaporation instrument AUTO 306 (from HHV Ltd., UK) at a pressure below 10^{-6} mbar. Immediately after the evaporation of metal layers, the slides were immersed overnight in a 1 mM solution of BP-S_2 in dimethyl sulfoxide (DMSO) to form a self-assembled monolayer (SAM). After rinsing with ethanol, 100 μL of a pNIPAAm terpolymer solution with concentrations from 0.5−2.5% (w/w) in pure ethanol was spun on top, at 2000 rpm for 120 s, using SpinCoatG3-P8, (from SCS, IN, USA). The polymer layer was subsequently dried at 50 °C in a vacuum oven for a minimum of 4 h and then irradiated with UV-light at 365 nm (UV lamp Bio-Link 365, Vilber Lourmat) with 2 J/cm^2 dose to cross-link and simultaneously attach the polymer to the surface. The layer thickness depends linearly on the concentration of the polymer solution spun on the surface.

Post-modification of HG Layers with Peptides. For the click coupling of alkyne-modified peptides to azide groups introduced to the HG network, copper-mediated cyclization[26] was used. First, the carboxyl groups in the pNIPAAm-based network were activated with EDC and TFPS for 15 min, washed with ACT buffer pH 5, and then exposed to 2.6 μM 2-azidoethan-1-aminium chloride in ACT pH 5 for 1 h. After washing, passivation was done with ethanolamine, continued by either drying and storage or using in experiments immediately after. For the attachment of peptides to the azide groups, a solution of 0.05 M $CuSO_4{\cdot}5H_2O$ in 3:1 DMSO/*t*-butanol and a solution of 0.05 M tris((1-benzyl-4-triazolyl)methyl)amine (TBTA) in 3:1 DMSO/*t*-butanol was mixed 1:2. To 1.5 μL of this solution, 0.75 μL of 0.1 M Na-ascorbate in water was added, as well as 2 μL of the peptide solution, which was dissolved in PBS at a stock concentration of 500 μM. 4.38 μL of DMSO and 1.37 μL of H_2O was added to a final volume of 10 μL. All reagents were freshly prepared. A volume of 7.5 μL was put onto the chip and allowed to react in the dark for 2 h, covered with a coverslip (20 × 20 mm). The chip was rinsed with water and PBS with 1 mg/mL BSA and 0.05% Tween (PBST).

For the spotting of peptides on microarrays, peptides dissolved to a concentration of 80 μM (from 500 μM stock in DMSO) in an aqueous buffer containing 10% DMSO, 1.25 mM Na-ascorbate, 1 mM hydroquinone, and 0.95 mM $CuSO_4$ (which equals to around 16 fmol of the peptide on each spot on which a volume of 0.2 nL was delivered) were degassed and microspotted by using the contactless spotter Marathon Argus (from Arrayjet, UK). The sensor chips were either directly used for further immunoassay experiments or stored in an argon atmosphere and preventing light exposure for up to several months without affecting its performance.

Post-modification of HG Layers with Antibodies. Carboxyl groups present in the pNIPAAm-based HG were activated using EDC and TFPS (21 and 75 mg, respectively) in 1 mL of water for 15 min. Immediately after washing with ACT buffer pH 4, IgG in ACT pH 4 was spotted using printer Omnigrid arrayer (from GeneMachines, San Carlos, CA, USA) with SMP 3 pins (from TeleChem International Inc., Sunnyvale, CA, USA) under adjusted air humidity (55−60%). Alternatively, the whole surface was brought in contact with the IgG solution and allowed to react for 1 h. After rinsing, the possible unreacted groups were passivated with 1 M ethanolamine pH 8.5 in water for 15 min and used for further assay experiments or stored at 4 °C in the dark in an argon atmosphere for several weeks without deterioration in the performance.

Optical Instruments. Two different readout methods were used in the course of the experiments (Figure 1). A PowerScanner (from Tecan, Switzerland) that utilizes the epi-illumination fluorescence (EPF) geometry was used for the scanning of arrays spots (endpoint measurements) (λ_{ex} = 635 nm, λ_{em} = 676 nm). *In situ* observation of the assay steps and layer modifications was done by an instrument built in-house. It relies on the Kretschmann configuration of attenuated total reflection and allows for combined readout based on SPR and PEF. Shortly, a He−Ne laser (2 mW) emitting at λ_{ex} = 632.8 nm was made passing through a laser bandpass filter (LBPF, Thorlabs, FL632.8-10), a chopper model 197 (from Signal Recovery, USA) set to frequency f = 933 Hz, and a polarizer (POL) and was coupled to a 90° prism made of high refractive index glass LASFN9 with an optically matched glass substrate (using immersion oil) carrying a thin gold layer. A flow cell made of a transparent glass substrate with drilled inlet and outlet ports was clamped on top of the substrates, which, for temperature-control, had a Peltier element as described previously.[12] A polydimethylsiloxane gasket (thickness: 100 μm; volume: 5 μL) and tubing Tygon LMT-55 (from Ismatec, Germany) with an inner diameter of 0.25 mm was used for the transportation of the liquids using a peristaltic pump (from Ismatec, Germany) at a flow rate of 15 μL/min. The intensity of the laser beam reflected at the sensor surface R was measured as a function of the angle of incidence θ or time t by a photodetector connected to a lock-in amplifier (from EG&G, USA). The enhanced field intensity associated with the resonant excitation of SPs was used for the excitation of Alexa Fluor 647 fluorophores. The emitted fluorescence light intensity F at the emission wavelength λ_{em} = 670 nm was detected by a photomultiplier tube (PMT, H6240-01, Hamamatsu, Japan) after a set of filters [laser notch filter (LNF) XNF-632.8-25.0M (from Melles Griot, CVI, USA) and 2 bandpass filter FBPF FB670-10 (from Thorlabs, USA) and 670FS10-25 (from Andover Corporation Optical Filter, USA)]. Both readout signals (reflectivity and fluorescence intensity changes) were recorded using Wasplas software developed at the Max Planck Institute for Polymer Research, Mainz, Germany.

Human IgG Detection by Peptide Ligands. Chips with a pNIPAAm-based HG layer were spotted with a pattern of alternating CA12 and EBV1-4 peptides (see above) and processed by blocking the surface with DIG easyHyb (Roche), washed two times for 15 min with a working PBS buffer with dissolved 0.05% Tween and 1 mg/mL BSA. Then, the surface was reacted with pooled hIgG at a concentration of 0.3 mg/mL (corresponding to 2 μM) for 1 h, followed by incubation with 2 μg/mL AF647 anti-hIgG (corresponding to 13 nM) for 45 min. After the rinsing and drying steps, the readout was done using the microarray scanner.

Observation of Thin HG Layer Swelling. Thin pNIPAAm-based HG layers were characterized by SPR to determine the dependence of the thickness d_h and the swelling ratio SR on temperature T in the range between 20 and 40 °C. The measured reflectivity spectra $R(\theta)$ were analyzed by fitting with a Fresnel reflectivity model implemented in software Winspall, developed at the Max Planck Institute for Polymer Research, Mainz, Germany. The method of matching the surface mass density measured in dry and

https://doi.org/10.1021/acsami.1c05950
ACS Appl. Mater. Interfaces 2021, 13, 27645−27655

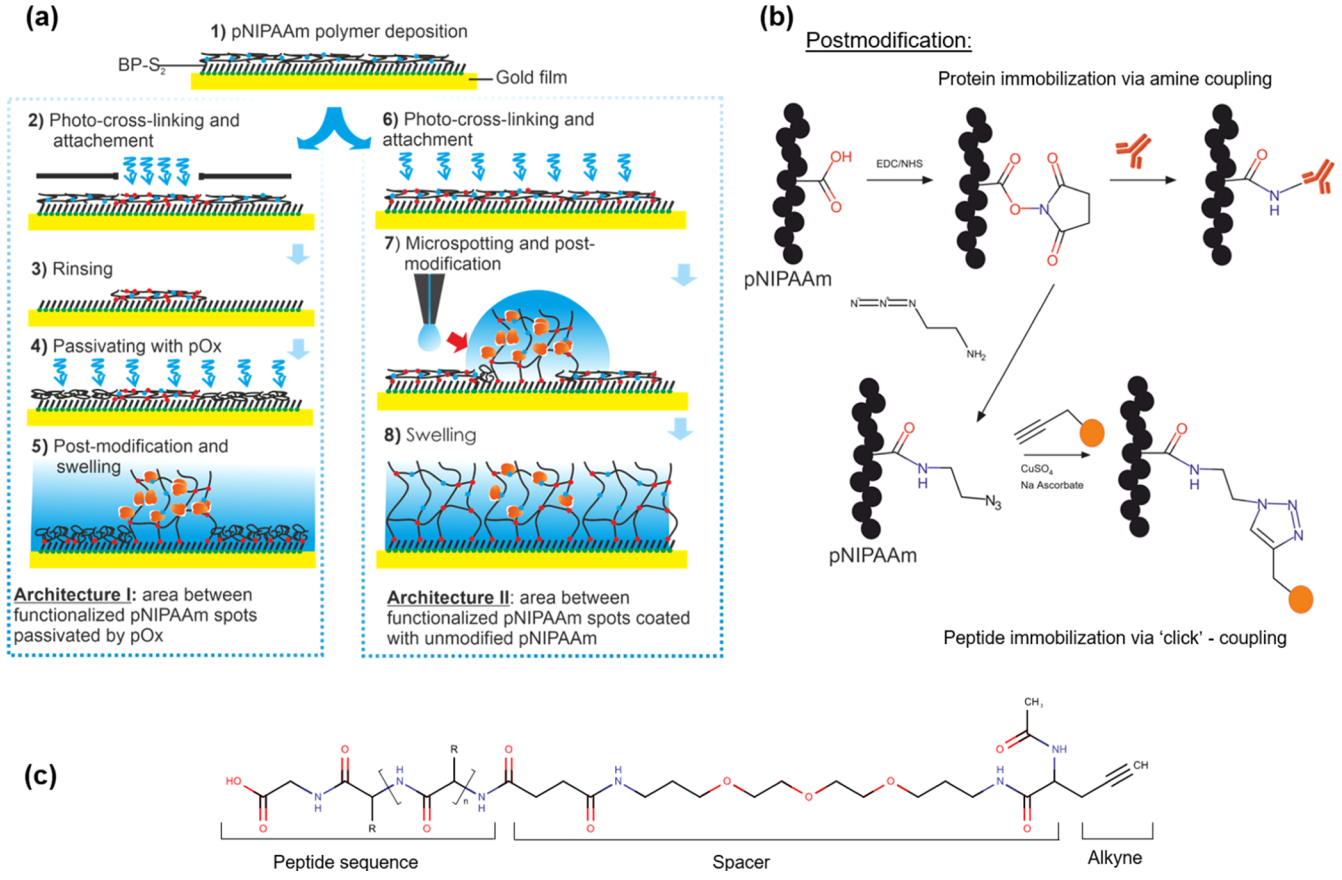

Figure 2. (a) Preparation routes for the microarrays with a pNIPAAm-based HG binding matrix. (b) Post-modification of pNIPAAm-based HG with protein and peptide molecules. (c) Structure of the used peptide ligands.

swollen states was used, and the SR was calculated as the ratio of the swollen film thickness to the dry film thickness (SR = $d_h/d_{h\text{-}dry}$).

Observation of the Assay in Biological Fluids by PEF. Thin HG layers bearing either no ligand or EBV4 peptide immobilized *via* click coupling (see above) were used for PEF detection. First, unspecific binding was tested with 2 μg/mL AF647 anti-hIgG, then human plasma diluted 1:10 in PBST was flowed over the surface for 30 min. After rinsing with PBST for 5 min, detection was performed for 15 min with 2 μg/mL AF647 anti-hIgG. Each step was observed and analyzed as described before.

RESULTS AND DISCUSSION

A tailored pNIPAAm-based HG was utilized in the form of a thin layer that was attached to a metallic sensor surface and post-modified with the antibody and peptide ligands for the affinity capture of target species. The analyte molecules captured from the analyzed aqueous sample at the sensor surface were then reacted with fluorophore-labeled detection antibody (dAb) in order to establish a sandwich assay format. The focused optical beam at the excitation wavelength of the fluorophore (λ_{ex}) was laterally scanned over the surface carrying arrays of sensing spots reacted with dAb, and the output fluorescent signal was collected at the fluorophore emission wavelength (λ_{em}) by an instrument relying on an epi-illumination configuration—EPF (Figure 1a). In order to observe the swelling of the HG layer in the direction perpendicular to the surface, the biochip surface was probed with the evanescent optical field at the fluorophore excitation wavelength λ_{ex}. Then, an optical setup that combines SPR and PEF was employed with an optical configuration resembling the TIRF (Figure 1b).

Preparation of Array HG Sensing Spots. The arrays of sensing spots were prepared using a polymer network formed by photocross-linking of a pNIPAAm-based terpolymer layer attached to a solid substrate (Figure 1c,d). The pNIPAAm-based layer exhibited a thickness of $d_{h\text{-}dry}$ = 120 nm in the dry state, and it was anchored atop of a glass substrate with a 50 nm thick gold film and BP-S_2 SAM (Figure 1d). As illustrated in Figure 2, BP-S_2 serves as a linker and two routes for the preparation of arrays of sensing spots were pursued, yielding either a laterally structured pNIPAAm-based HG layer conjugated with ligands (surface architecture I) or a continuous pNIPAAm-based HG layer that was locally post-modified with ligands by using microspotting (surface architecture II). The used pNIPAAm-based HG was allowed to swell in water after its preparation, yielding a thickness of d_h = 700 nm (as demonstrated by the following SPR study) corresponding to a swelling ratio SR = $d_h/d_{h\text{-}dry}$ of 5.8.

In the first route toward surface architecture I, the deposited pNIPAAm-based polymer was cross-linked by UV light through a stencil mask with square arrays of circular apertures exhibiting a diameter of 500 μm and a period of 800 μm. An irradiation dose of 2 J/cm^2 was used to simultaneously cross-link and attach the polymer chains to the gold surface by the photoactivated benzophenone groups carried by their backbone and by the BP-S2 linker on the gold surface (Figure 2a, step 2). After rinsing with ethanol (Figure 2a, step 3), the pNIPAAm polymer chains outside the irradiated zones were washed away, leaving the surface with unreacted BP-S_2. To

https://doi.org/10.1021/acsami.1c05950
ACS Appl. Mater. Interfaces 2021, 13, 27645−27655

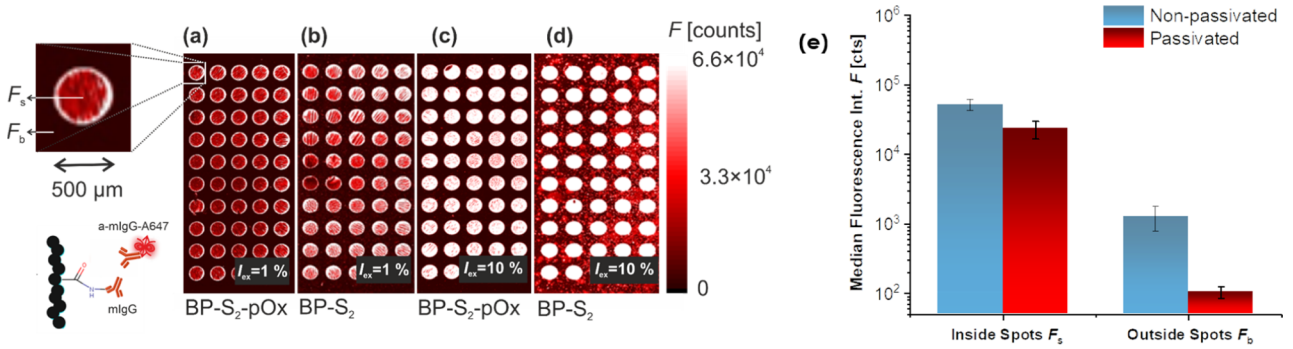

Figure 3. Fluorescence images of biochip architecture I acquired by EPF: (a,c) arrays with a pOx-passivated area between the sensing spots and (b,d) arrays without the pOx passivation. The images were measured (a,b) with the excitation power I_{ex} = 1% and (c,d) with the excitation power I_{ex} = 10%. (e) Comparison of the average fluorescence intensities F_s and F_b for excitation power I_{ex} = 1%.

protect this hydrophobic area and thus prevent the unspecific adsorption of biomolecules from the analyzed samples, a thin layer of noncross-linkable pOx was coupled on these zones. This polymer was deposited over the whole biochip surface area, followed by the irradiation with UV light (Figure 2a, step 4) upon which the pOx polymer chains in contact with BP-S_2 attached to the gold surface. After additional rinsing of the surface, the pOx on the already coated sensing spots and further away from the gold surface was washed away. Therefore, pOx forms a thin monolayer only outside the circular sensing spots where its chains are in direct contact with the BP-S_2. Also, it is worth noting that the thin pOx "grafted to" polymer brush layer does not form a network as its polymer backbone does not carry benzophenone groups. Such an architecture was then used for the post-modification with functional biomolecules serving as ligands (Figure 2a, step 5). It is utilized for protein ligands by using amine-coupling through reacting carboxyl groups with EDC and TFPS. In addition, the coupling of peptide ligands carrying alkyne tags was performed by converting the carboxyl groups on the pNIPAAm-based polymer chains to azide moieties with amine−azide (Figure 2b). As only the pNIPAAm-based polymer carrying carboxylic groups is employed for the post-modification, the anchoring of the antibody or peptide ligands does not occur on the zones outside the sensing spots with pOx moieties.

In the second route toward architecture II, the whole pNIPAAm-based polymer layer was uniformly cross-linked with UV light using the same dose of 2 J/cm^2, followed by rinsing of loosely bound polymer chains (Figure 2a, step 6). Then, the carboxylic groups present in the photocross-linked pNIPAAm-based polymer networks were activated by EDC and TFPS, and the functional biomolecules were immobilized inside the polymer networks in defined, spatially controlled areas by microspotting (Figure 2a, step 7). After the subsequent rinsing and passivating the remaining activated carboxyl groups with ethanolamine, the HG film was swollen, yielding arrays of functional molecules attached to flexible polymer chains inside the pNIPAAm-based networks (Figure 2a, step 8).

Observation of Affinity Binding with Architecture I. The arrays of sensing spots were *in situ* post-modified with an antibody ligand (mouse immunoglobulin G—mIgG) and were allowed to bind its affinity partner that was labeled with a fluorophore (anti-mIgG-AF647). For the used concentration of 12 nM and a time of 45 min, the affinity reaction reached saturation, and the majority of accessible mIgG binding sites inside the HG was assumed to bind with anti-mIgG-AF647. After the washing and drying steps, the fluorescence images were acquired with the EPF geometry by scanning the excitation beam at λ_{ex} = 635 nm over the arrays and recording the fluorescent signal F emitted at λ_{em} = 670 nm.

The acquired fluorescence images are presented in Figure 3, and they show a series of bright spots with a size of 500 μm that correspond to the HG-coated zones where the a-mIgG-AF647 biomolecules were affinity captured to covalently coupled mIgG. As shown in the inset of Figure 3a, fluorescence intensity inside the spots is homogeneously distributed, and one can observe a brighter rim at their circumference. This can be attributed to the possible lateral swelling of the cylindrically shaped HG coating at the sensing spots occurring at its vertically oriented walls (besides the swelling in the perpendicular direction at the horizontally oriented interfaces, which is investigated by SPR further). This effect may enhance the accessibility of the binding sites and locally increase the amount of captured biomolecules. The averaged fluorescent signal from inside the spots F_s and outside the spots F_b was compared for biochip architecture I with the pOx passivation (a,c) and without the passivation (b,d). The excitation beam power was set to either 1% (a,b) or 10% (c,d) to distinguish the weaker background fluorescence intensity originating from outside the spots F_b. For a lower excitation power of 1%, the fluorescence intensity collected from inside the spots F_s was about 50% lower on the chip with the pOx passivation than that without (F_s = 23,000 *vs* 50,000 counts). This can be attributed to the hindered diffusion of biomolecules through the HG due to the higher cross-linking density associated with the double exposure to UV light. For the stronger excitation power I_{ex} = 10%, the fluorescent signal F_s was above the saturation level (Figure 3c,d).

The fluorescent signal in the area between the sensing spots F_b originates from the unspecific physisorption of the ligands upon the post-modification step and the subsequent affinity binding and/or physisorption of anti-mIgG-AF647. These effects are particularly pronounced for the hydrophobic surface of the BP-S2 SAM and are substantially suppressed by the pOx passivation. The obtained data confirmed that the background signal F_b outside the spots decreased by more than 1 order of magnitude when the pOx passivation was used (F_b = 100 *vs* 1200 counts for the excitation power I_{ex} = 1%). This difference is clearly visually observed from the images acquired for the increased excitation power of 10%.

In order to quantify the quality of the biointerface in fluorescent microarrays, the signal-to-noise ratio (SNR) is

https://doi.org/10.1021/acsami.1c05950
ACS Appl. Mater. Interfaces 2021, 13, 27645−27655

often used. It is defined as SNR = $F_s - F_b/\sigma(F_b)$, where $\sigma(F_b)$ states for the standard deviation of the background signal.[27] The SNR in the field of microarrays is affected by the surface chemistry utilized for the spotting (e.g., epoxy, nitrocellulose, and HG) as well as the deviations occurring during all preparation, hybridization, and scanning steps. Usually, an SNR above 3 is considered as a useable threshold[28] and, here, the values of 1160 and 104 are obtained for the pOx-passivated and nonpassivated surfaces, respectively, when the excitation power was set to I_{ex} = 1%.

Observation of Affinity Binding with Architecture II. The EPF readout was also employed to characterize spatially controlled affinity binding on biochip architecture II by using the same immunoassay. Here, the mIgG serving as the ligand was delivered onto a series of sensing spots by using microspotting with a tip that dispenses a 0.7 nL liquid volume over the pNIPAAm-based photocross-linked layer with the carboxylic groups pre-activated by EDC and TFPS. The concentration of the mIgG serving as the ligand in the spotted droplets was set in the range from 0 to 3 μM, and the microspotted arrays were arranged in a lattice with a period of 300 μm.

After the affinity binding of anti-mIgG-AF647 to the covalently immobilized mIgG (following the same protocol as for architecture I), the biochip was rinsed, dried, and the fluorescence intensity images were acquired. As Figure 4a shows a series of bright fluorescence spots are observed due to the affinity binding in the spotted areas, and the diameter of each spot was about 100 μm. The acquired intensity exhibits maximum in the middle of the spot, and it decreases when moving away from its center (which gives the impression of decreasing spot area with decreasing mean intensity F_s). It also illustrates the dependence of the mean intensity F_s and F_b on the microarray scanner settings, either in a high dynamic range (left) or with a high gain (right). Figure 4b shows the fluorescence signal intensity F_s from the affinity-bound a-mIgG-A647 depending on the concentration of the mIgG ligand used for the microspotting and covalent coupling to pNIPAAm-based polymer chains. It reveals that above mIgG concentration of 1 μM, the response F_s flattens as all available activated carboxyl groups in the pNIPAAm-based HG layer were used for the amine coupling of the ligand. However, the fluorescence intensity F_s reaches the reader saturation values for a more than one order of magnitude higher excitation power of I_{ex} = 50% compared to the architecture II (when the scanner is set for high gain). This observation indicates that the microspotting protocol used in the architecture II provides lower immobilization yield than the *in situ* incubation in architecture I and thus, deteriorated SNR varying between 20 and 250 was achieved.

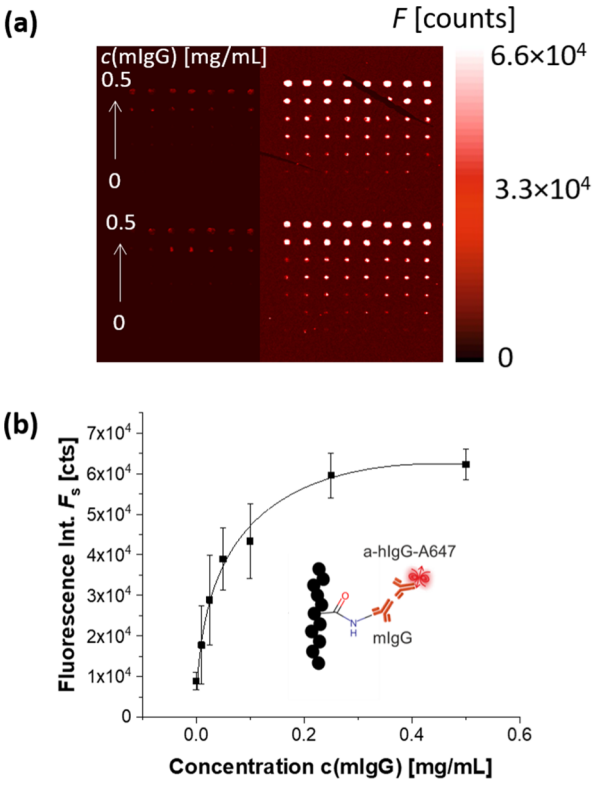

Figure 4. (a) Fluorescence observation of architecture II acquired by EPF with varying concentrations of spotted mIgG after incubation with fluorescently labeled anti-mIgG-AF647 dissolved at 12 nM concentration. 50% laser intensity and scanner configured for high (left) and low (right) dynamic ranges. (b) Comparison of the fluorescence intensity emitted from the sensing spots F_s after the assay with the scanner set to the high dynamic range. The error bars represent the standard deviation of the eight spots for each concentration.

Nevertheless, architecture II allows a straightforward immobilization of different ligands in the array format and thus, it is further exploited for the spotting of four peptides with sequences derived from the EBV antigen (EBV1-4)[29] together with the control CA12 peptide derived from the enzyme carbonic anhydrase XII. These peptides were spotted by dispensing 0.2 nL of a solution spiked with each peptide ligand at a concentration of 80 μM on the pNIPAAm-based polymer layer. Before the microspotting, the carboxylic groups carried by the pNIPAAm-based polymer chains were converted to azide groups (Figure 2b), so the peptides bearing a propargylglycine (alkyne) side group can covalently couple by a copper-mediated click reaction. The prepared peptide microarrays were employed to detect human IgG (hIgG) collected from blood donors' plasma, reactive against the EBV. In this experiment, the sensor chip was sequentially exposed to isolated hIgG dissolved at a concentration of 0.3 mg/mL (2 μM) followed by the binding of captured hIgG with anti-hIgG conjugated with AF647 (13 nM). Figure 5 summarizes the

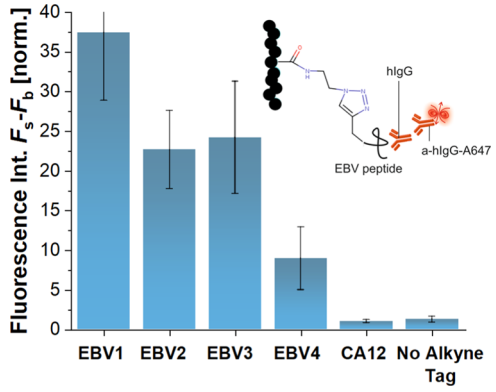

Figure 5. Fluorescence intensities for architecture II after the affinity capture of hIgG pooled with known reactivity against EBV followed by tagging with the fluorescently labeled secondary antibody in comparison with the control CA12. All values are relative to an untagged peptide.

https://doi.org/10.1021/acsami.1c05950
ACS Appl. Mater. Interfaces 2021, 13, 27645−27655

results and reveals that the spots with the specific peptides EBV1-4 show a 9 to 30-fold stronger fluorescent signal F_s in comparison to the control spots with the CA12 peptide and bare pNIPAAm-based polymer network (where peptides without the alkyne tag were spotted).

Furthermore, the performance of the peptide arrays prepared on the 3D pNIPAAm-based HG film was compared to that on the commercial substrate carrying the 2D monolayer interface with azide groups (2D-Azide from PolyAn, Germany). Under identical conditions as in the previous experiments presented in Figure 5, antigenic peptide EBV4 with an alkyne group on either the C or N terminus was spotted onto both interfaces of commercial 2D-Azide and of 3D pNIPAAm-based HG that was post-modified with an 2-azidoethan-1-aminium chloride. As a mock control, there was also spotted EBV4 peptide with a biotin end group. Figure 6

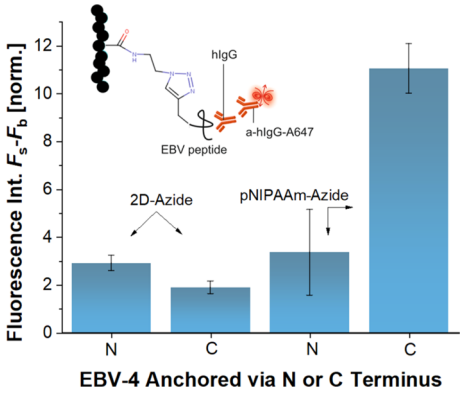

Figure 6. Fluorescence intensities relative to biotin control for architecture II after the affinity capture of hIgG pooled with known reactivity against EBV4 followed by tagging with a fluorescently labeled secondary antibody for commercial 2D-Azide slides (PolyAn) and 3D HG slides, with the alkyne tag bound to either N or C terminus of the peptide.

shows that specific fluorescent signal F_s-F_b acquired on the 2D-Azide slides carrying the EBV4 peptide immobilized *via* the N and C terminus was higher by a factor of 1.8 and 2.7, respectively, with respect to that for the mock control. Such moderate signal strength suggests that the peptide with the biotin tag was probably also partially immobilized onto the control spots carried by the 2D-Azide surface. Importantly, a stronger signal increase of 6 and 10-fold was measured for the EBV4 peptide immobilized *via* the N and C terminus, respectively, on the 3D pNIPAAm-based HG when compared to the mock control.

Interestingly, the peptide orientation clearly affected the fluorescence response on a HG matrix as a 3-fold higher signal was measured for the C-terminal bound peptide compared to the N-terminal one. This is different for the 2D-Azide surface, and it can be ascribed to the effect of steric hindrance that is partially elevated when ligands are conjugated to flexible polymer chains forming the HG interface. When comparing the SNR, a value of 67 was obtained for the 2D-Azide slides, and a slightly better SNR of 88 was determined for the 3D pNIPAAm-based HG matrix. In a nutshell, these experiments confirm an enhanced signal and a possible implementation of assays utilizing both amine coupling and click chemistry for the conjugation of protein as well as peptide ligands, respectively, to the pNIPAAm-based polymer network that can then serve as a binding matrix.

Dual Amplification of the Fluorescent Signal—Plasmonic Excitation and Temperature-Induced Collapse. The responsive properties of the pNIPAAm-based HG matrix offer additional means to manipulate the captured target molecules by exploiting its temperature-induced collapse. Upon pNIPAAm-based HG compaction occurring above its LCST, the affinity-captured biomolecules inside the polymer network structure are dragged toward the gold surface, as shown in Figure 7a. Then, the fluorophore labels bound in the

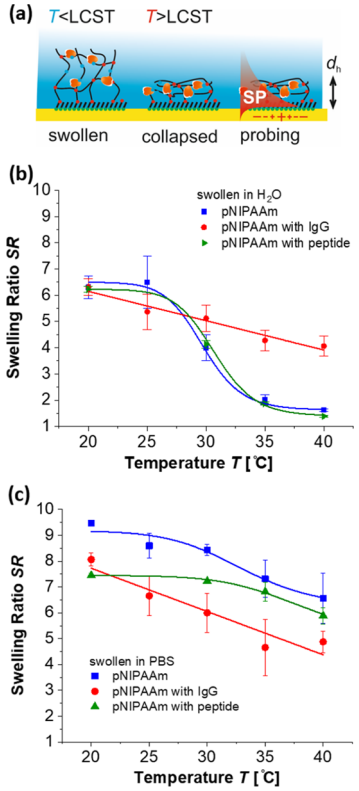

Figure 7. (a) Schematic of the SPR probing of swelling changes and responsive properties of the pNIPAAm-based HG in contact with (b) H_2O and (c) PBS that is affected by the post-modification with high (mIgG)- and low (peptide)-molecular-weight ligands. Swelling ratios are derived from the SPR signal and are fitted with the sigmoidal function (lines) (obtained error bars are derived from standard deviation of the SR).

HG matrix after the specific capture of the target analyte can be placed at the optimum distance from the metal surface in order to benefit from the optical amplification based on PEF.[30] This amplification originates from the probing by the confined field of increased intensity of SPs, which translates to the enhanced fluorescence emission rate without changing the background signal.

To utilize this concept, we first characterized changes in the responsive properties of the pNIPAAm-based HG layer after its post-modification with the high-molecular-weight IgG ligand (MW = 160 kDa) and smaller peptide ligand (MW = 2.3 kDa). The thickness of the HG layer d_h was measured as a function of temperature T by using SPR.[12] As shown in Figure 7b, the measured changes in the HG layer thickness d_h were normalized with that obtained for a dry polymer film $d_{h\text{-}dry}$ to yield to swelling ratio SR = $d_h/d_{h\text{-}dry}$. For the pristine

https://doi.org/10.1021/acsami.1c05950
ACS Appl. Mater. Interfaces 2021, 13, 27645−27655

pNIPAAm-based HG in contact with water, the HG layer collapses at a temperature between T = 30 and 35 °C, which is in agreement with the pNIPAAm LCST of 32 °C. The swelling ratio SR correspondingly drops by a factor of 4.7 when increasing the temperature from T = 20 to 40 °C. The response of the pNIPAAm-based HG to temperature changes is strongly suppressed after its post-modification with IgG molecules as the SR changed only by a factor of 1.6 when increasing the temperature from T = 20 to 40 °C. This observation agrees with our previous study, and it can be ascribed to the hydrophilic nature of IgG that dominates over the properties of pNIPAAm polymer networks when switched to a hydrophobic state above the LCST.[17] Importantly, the response of the same HG layer that was post-modified with a lower molecular weight peptide EBV4 (MW = 2.3 kDa) is preserved as the swelling ratio SR changes by a factor of 4.3 when increasing temperature T from 20 to 40 °C. This change is similar to that observed for the pristine pNIPAAm HG layer in contact with water. However, the thermoresponsive characteristics are strongly suppressed when it is swollen in PBS. Like in our previous studies, the swelling ratio SR gradually decreases with the increase of temperature T from 20 to 40 °C by only a small factor of about 1.5, which can be ascribed to the presence of ions in the solution.[31]

Finally, the peptide-functionalized pNIPAAm-based binding matrix was explored for the affinity capture of the target analyte from the pooled human plasma and for its detection by using a dual amplification strategy. The affinity captured hIgG against EBV was compacted at the sensor surface using a temperature stimulus, and the surface plasmon-enhanced fluorescence was used for its detection. In this experiment, the sensor chip with the pNIPAAm-based HG was attached atop of a glass substrate with a 50 nm thick gold layer, and it was post-modified with the EBV4 peptide. The thickness of the HG was set to $d_{\text{h-dry}}$ = 40 nm in order to match with the penetration depth of the probing field of resonantly excited SPs (about 100 nm). The sensor chip was then loaded to an optical system for the combined SPR and PEF measurements. In the PEF modality, the excitation of the fluorescent signal was utilized *via* the enhanced field intensity of the SPs at the fluorophore excitation wavelength λ_{ex}. In the used system, the resonant coupling to SPs was tuned by varying the angle of incidence θ and it is manifested as a dip in the reflectivity spectrum $R(\theta)$ and respective peak in the fluorescence intensity spectrum $F(\theta)$, as shown in Figure 8.

The swollen HG film carrying immobilized EBV4 peptides was reacted with a pooled human plasma, diluted 1:10 in PBST buffer. The whole concentration of hIgG in the plasma is around 8.5 mg/mL,[32] and a small fraction is specific to EBV. First, the surface of pristine (unmodified) pNIPAAm-based HG with no peptide ligand immobilized was exposed to the pooled human plasma (diluted with PBS 1:10) followed by the reaction with the detection antibody a-hIgG-A647 for 15 min at a concentration of 13 nM. Afterward, the same experiment was performed for the pNIPAAm-based HG that was post-modified with the EBV4 peptide. After each step, the reflectivity scan $R(\theta)$ was measured together with the fluorescence intensity spectrum $F(\theta)$. As shown in Figure 8b, the affinity binding of hIgG against EBV is manifested as a peak in the fluorescence angular spectrum $F(\theta)$ located close to the angle θ where the resonance excitation of SPs occurs [manifested as a dip in the respective $R(\theta)$]. These graphs reveal that increasing the temperature from T = 25 to 40 °C

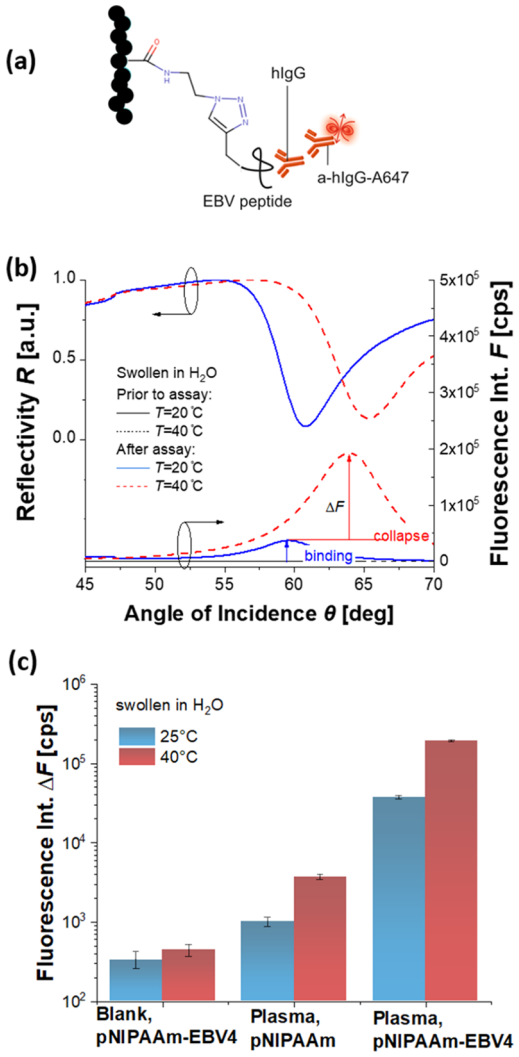

Figure 8. (a) Schematics of the sandwich assay with the peptide ligand in the thermoresponsive pNIPAAm-based binding matrix. (b) Angular reflectivity and fluorescence intensity scans at temperatures of T = 25 and 40 °C before and after the assay, a-EBV antibodies from the diluted human plasma, followed by anti-hIgG-AF647. (c) Comparison of the peak fluorescence intensities of only anti-hIgG-AF647, unspecific binding of plasma to the HG without a ligand, and specific detection of a-EBV antibodies in the plasma through the peptide assay, both for swollen and collapsed states of the HG binding matrix. Error bars were determined as 3× the standard deviation of the fluorescent signal.

leads to a shift in the SPR reflectivity dip by about 5° due to the increase of the refractive index on the gold surface associated with the collapse of the polymer network. Notably, the fluorescence peak also shifts by the same angle, and its peak intensity increases by a factor of 5 for the affinity capture of hIgG against EBV in water. This additional enhancement can be attributed to the dragging of target molecules closer to the gold surface, where the maximum plasmonic enhancement occurs. The summary of the peak fluorescence intensities ΔF presented in Figure 8c compares the signal acquired for control experiments and the specific detection of a-EBV antibody. In the first control, a nonmodified HG was directly reacted with detection antibody a-hIgG-A647 and its unspecific sorption leads to an increase of the fluorescent signal of about ΔF = 600 cps. The same was done for the EBV4 peptide-modified HG

https://doi.org/10.1021/acsami.1c05950
ACS Appl. Mater. Interfaces 2021, 13, 27645−27655

layer as a second control, which showed an even lower increase of ΔF = 300 cps. The third control was performed in the nonmodified HG layer exposed to 10% pooled human plasma followed by reacting with detection antibody a-hIgG-A647, which showed a higher response of $\Delta F = 10^3$ cps. Finally, the specific detection of a-EBV antibodies in 10% pooled plasma was tested and revealed a strong signal of $\Delta F = 3 \times 10^4$ cps at room temperature T = 25 °C. From the angular scans, $F(\theta)$ follows that the peak fluorescent signal further increases by a factor of 5 to $\Delta F = 1.5 \times 10^5$ cps, when the temperature is changed from T = 25 °C to 40 °C and the pNIPAAm-based HG collapses at the metallic surface. From these data, no apparent fluorescent background signal due to the autofluorescence of the pNIPAAm network itself was observed and when calculating the SNR ratio (analogously as on the microarray experiments above), a value of 1550 and 8000 was determined for 25 and 40 °C, respectively, highlighting the advantage of a dual amplification approach.

CONCLUSIONS

A thin responsive HG layer was tailored to serve as an affinity binding matrix in assays with a fluorescence readout, and its utilization to dual amplification strategy was explored. It is based on the combination of optical enhancement and efficient pre-concentration of captured analytes by the HG compaction triggered by an external stimulus. This concept was carried out using a pNIPAAm-based terpolymer with functional and photoreactive groups, allowing the facile post-modification by ligand molecules and photocross-linking and patterning arrays of sensing spots. Antibody and peptide ligands were conjugated with the pNIPAAm-based three-dimensional polymer network through amine and click coupling, respectively, for the specific capture of target biomolecules. The ability to perform analysis in complex samples is demonstrated by the detection of human IgG against EBV in the human plasma with a set of peptide ligands. The developed responsive biointerface is documented to provide improved performance characteristics with respect to commercial sensor chips with azide groups arranged in a regular two-dimensional architecture.

The pNIPAAm-based thermoresponsive biointerface platform was employed on a sensor chip for surface plasmon-enhanced fluorescence measurements, which in conjunction with specific metallic nanostructures can provide optical enhancement in the acquired fluorescent signal by a factor of 300.[30,33] Compared to our previous studies with large-molecular-weight antibody ligands,[17] post-modification with low-molecular-weight peptides offers the advantage of preserving the thermoresponsive properties of pNIPAAm-based polymer networks, and it translates into a pronounced increase in the fluorescence intensity by a large factor of 5. The combination of optical- and analyte-compaction-based amplification holds the potential to benefit from both the high binding capacity of the swollen HG binding matrix and probing with the tightly confined electromagnetic field associated with the excitation of SPs on metallic thin films and nanostructures. It can provide a route for efficient *in situ* fluorescence measurements with the combined enhancement factor >10^3 under realistic conditions and complex samples. Moreover, new sensor modalities can be developed for rapid and sensitive fluorescence monitoring of biomolecular binding events and affinity interactions in conjunction with fast temperature actuation, which for instance, is possible by plasmonic heating.[34]

ASSOCIATED CONTENT

Supporting Information

The Supporting Information is available free of charge at https://pubs.acs.org/doi/10.1021/acsami.1c05950.

IR spectrum and ^{1}H and ^{13}C NMR spectra of 2-azidoethylamine, ^{1}H and ^{13}C NMR spectra of benzophenone disulfide, ^{1}H NMR spectra of 4-benzophenylacrylamide and the pNIPAAm-based terpolymer, and comparison of ^{1}H NMR spectra of the terpolymer and pOx (PDF)

AUTHOR INFORMATION

Corresponding Author

Jakub Dostalek − *Biosensor Technologies, AIT-Austrian Institute of Technology GmbH, Tulln an der Donau 3430, Austria; FZU-Institute of Physics, Czech Academy of Sciences, Prague 182 21, Czech Republic;* orcid.org/0000-0002-0431-2170; Phone: +43 (0) 50550 4470; Email: jakub.dostalek@ait.ac.at; Fax: +43 (0) 50550 4450

Authors

Simone Hageneder − *Biosensor Technologies, AIT-Austrian Institute of Technology GmbH, Tulln an der Donau 3430, Austria;* orcid.org/0000-0002-7200-3257

Vanessa Jungbluth − *Biosensor Technologies, AIT-Austrian Institute of Technology GmbH, Tulln an der Donau 3430, Austria;* Present Address: Dipartimento di Scienze Chimiche, Università degli Studi di Catania, Catania, Italy.; orcid.org/0000-0002-3176-2839

Regina Soldo − *Molecular Diagnostics, Health & Environment, AIT Austrian Institute of Technology GmbH, Vienna 1210, Austria;* Present Address: Greiner Bio-One, Greinerstraße 70, Kremsmünster, Austria.

Christian Petri − *Macromolecular Chemistry, Department Chemistry—Biology, University of Siegen, Siegen 57076, Germany*

Matthias Pertiller − *Biosensor Technologies, AIT-Austrian Institute of Technology GmbH, Tulln an der Donau 3430, Austria;* orcid.org/0000-0002-6315-2306

Marjut Kreivi − *Ginolis Ltd, Oulunsalo 90460, Finland;* Present Address: VTT-Technical Research Centre of Finland, Kaitoväylä 1, Oulu FIN-90590, Finland.; orcid.org/0000-0002-6288-2155

Andreas Weinhäusel − *Molecular Diagnostics, Health & Environment, AIT Austrian Institute of Technology GmbH, Vienna 1210, Austria*

Ulrich Jonas − *Macromolecular Chemistry, Department Chemistry—Biology, University of Siegen, Siegen 57076, Germany;* orcid.org/0000-0002-2161-4541

Complete contact information is available at: https://pubs.acs.org/10.1021/acsami.1c05950

Notes

The authors declare no competing financial interest.

ACKNOWLEDGMENTS

All the authors received support from the European Union's Horizon 2020 research and innovation program under grant agreement no. 633937, project ULTRAPLACAD. Additionally,

S.H. and J.D. were partially supported by the Austrian Research Promotion Agency (FFG) with grant agreement no. 861578 (ERANET project PLABAN) and by the Lower Austria project IKTHEUAP number WST3-F-5030820/010-2019. J.D. acknowledges support from the ESIF and MEYS (Project "FZU researchers, technical and administrative staff mobility"—CZ.02.2.69/0.0/0.0/18_053/0016627).

■ ABBREVIATIONS

EDC, 1-ethyl-3-(3-dimethylaminopropyl)carbodiimide
TFPS, 4-sulfotetrafluorophenol
ACT, acetate buffer
DCM, dichloromethane
DMSO, dimethyl sulfoxide
EBV, Epstein−Barr virus
FBPF, fluorescence bandpass filter
HG, hydrogel
IgG, immunoglobulin G
LNF, laser notch filter
LCST, lower critical solution temperature
MW, molecular weight
PEF, plasmon-enhanced fluorescence
pNIPAAm, poly(*N*-isopropylacrylamide)
PBS, phosphate-buffered saline
SAM, self-assembled monolayer
SNR, signal-to-noise ratio
SPR, surface plasmon resonance
TM, transverse magnetic
TBTA, tris((1-benzyl-4-triazolyl)methyl)amine

■ REFERENCES

(1) Mesch, M.; Zhang, C.; Braun, P. V.; Giessen, H. Functionalized Hydrogel on Plasmonic Nanoantennas for Noninvasive Glucose Sensing. *ACS Photonics* **2015**, *2*, 475−480.
(2) Jiang, Y.; Colazo, M. G.; Serpe, M. J. Poly(N-isopropylacrylamide) microgel-based etalons for the label-free quantitation of estradiol-17β in aqueous solutions and milk samples. *Anal. Bioanal. Chem.* **2018**, *410*, 4397−4407.
(3) Manikas, A. C.; Aliberti, A.; Causa, F.; Battista, E.; Netti, P. A. Thermoresponsive PNIPAAm Hydrogel Scaffolds with Encapsulated AuNPs Show High Analyte-Trapping Ability and Tailored Plasmonic Properties for High Sensing Efficiency. *J. Mater. Chem. B* **2015**, *3*, 53−58.
(4) Hilber, W. Stimulus-Active Polymer Actuators for next-Generation Microfluidic Devices. *Appl. Phys. A: Mater. Sci. Process.* **2016**, *122*, 751.
(5) Choe, A.; Yeom, J.; Shanker, R.; Kim, M. P.; Kang, S.; Ko, H. Stretchable and Wearable Colorimetric Patches Based on Thermoresponsive Plasmonic Microgels Embedded in a Hydrogel Film. *NPG Asia Mater.* **2018**, *10*, 912−922.
(6) Elashnikov, R.; Mares, D.; Podzimek, T.; Švorčík, V.; Lyutakov, O. Sandwiched Gold/PNIPAm/Gold Microstructures for Smart Plasmonics Application: Towards the High Detection Limit and Raman Quantitative Measurements. *Analyst* **2017**, *142*, 2974−2981.
(7) Álvarez-Puebla, R. A.; Contreras-Cáceres, R.; Pastoriza-Santos, I.; Pérez-Juste, J.; Liz-Marzán, L. M. Au@pNIPAM Colloids as Molecular Traps for Surface-Enhanced, Spectroscopic, Ultra-Sensitive Analysis. *Angew. Chem., Int. Ed.* **2009**, *48*, 138−143.
(8) Mueller, M.; Tebbe, M.; Andreeva, D. V.; Karg, M.; Alvarez Puebla, R. A.; Pazos Perez, N.; Fery, A. Large-Area Organization of PNIPAM-Coated Nanostars as SERS Platforms for Polycyclic Aromatic Hydrocarbons Sensing in Gas Phase. *Langmuir* **2012**, *28*, 9168−9173.
(9) Tokarev, I.; Tokareva, I.; Minko, S. Optical Nanosensor Platform Operating in Near-Physiological Ph Range via Polymer-Brush-Mediated Plasmon Coupling. *ACS Appl. Mater. Interfaces* **2011**, *3*, 143−146.
(10) Quilis, N. G.; Hageneder, S.; Fossati, S.; Auer, S. K.; Venugopalan, P.; Bozdogan, A.; Petri, C.; Moreno-Cencerrado, A.; Toca-Herrera, J. L.; Jonas, U.; Dostalek, J. UV-Laser Interference Lithography for Local Functionalization of Plasmonic Nanostructures with Responsive Hydrogel. *J. Phys. Chem. C* **2020**, *124*, 3297−3305.
(11) Heskins, M.; Guillet, J. E. Solution Properties of Poly(N-Isopropylacrylamide). *J. Macromol. Sci., Part A: Pure Appl.Chem.* **1968**, *2*, 1441.
(12) Aulasevich, A.; Roskamp, R. F.; Jonas, U.; Menges, B.; Dostálek, J.; Knoll, W. Optical Waveguide Spectroscopy for the Investigation of Protein-Functionalized Hydrogel Films. *Macromol. Rapid Commun.* **2009**, *30*, 872−877.
(13) Zhang, Q.; Wang, Y.; Mateescu, A.; Sergelen, K.; Kibrom, A.; Jonas, U.; Wei, T.; Dostalek, J. Biosensor based on hydrogel optical waveguide spectroscopy for the detection of 17β-estradiol. *Talanta* **2013**, *104*, 149−154.
(14) Andersson, O.; Larsson, A.; Ekblad, T.; Liedberg, B. Gradient Hydrogel Matrix for Microarray and Biosensor Applications: An Imaging SPR Study. *Biomacromolecules* **2009**, *10*, 142−148.
(15) Wang, Y.; Brunsen, A.; Jonas, U.; Dostálek, J.; Knoll, W. Prostate Specific Antigen Biosensor Based on Long Range Surface Plasmon-Enhanced Fluorescence Spectroscopy and Dextran Hydrogel Binding Matrix. *Anal. Chem.* **2009**, *81*, 9625−9632.
(16) Huang, C.-J.; Jonas, U.; Dostálek, J.; Knoll, W. Biosensor Platform Based on Surface Plasmon-Enhanced Fluorescence Spectroscopy and Responsive Hydrogel Binding Matrix. *Optical Sensors*; International Society for Optics and Photonics, 2009; Vol. *7356*; p 735625.
(17) Toma, M.; Jonas, U.; Mateescu, A.; Knoll, W.; Dostalek, J. Active Control of SPR by Thermoresponsive Hydrogels for Biosensor Applications. *J. Phys. Chem. C* **2013**, *117*, 11705−11712.
(18) King, P. J. S.; Saiani, A.; Bichenkova, E. V.; Miller, A. F. A de novo self-assembling peptide hydrogel biosensor with covalently immobilised DNA-recognising motifs. *Chem. Commun.* **2016**, *52*, 6697−6700.
(19) Liu, Q.; Wang, J.; Boyd, B. J. Peptide-Based Biosensors. *Talanta*. Elsevier B.V. May 1, 2015, *136*; pp 114−127. DOI: DOI: 10.1016/j.talanta.2014.12.020.
(20) Waheed, A.; Sly, W. S. Carbonic Anhydrase XII Functions in Health and Disease. *Gene*. Elsevier B.V. August 5, 2017, *623*, pp 33−40. DOI: DOI: 10.1016/j.gene.2017.04.027.
(21) Blake, S.; Capone, R.; Mayer, M.; Yang, J. Chemically Reactive Derivatives of Gramicidin A for Developing Ion Channel-Based Nanoprobes. *Bioconjugate Chem.* **2008**, *19*, 1614−1624.
(22) Gee, K. R.; Archer, E. A.; Kang, H. C. 4-Sulfotetrafluorophenyl (STP) Esters: New Water-Soluble Amine-Reactive Reagents for Labeling Biomolecules. *Tetrahedron Lett.* **1999**, *40*, 1471−1474.
(23) Sergelen, K.; Petri, C.; Jonas, U.; Dostalek, J. Free-Standing Hydrogel-Particle Composite Membrane with Dynamically Controlled Permeability. *Biointerphases* **2017**, *12*, 051002.
(24) Petri, C. *Synthesis and Characterization of Novel Photocrosslinkable Poly (2-Oxazoline)-Based Hydrogel Systems for the Application as Biosensor Matrix*; Universität Siegen, 2018.
(25) Tauhardt, L.; Frant, M.; Pretzel, D.; Hartlieb, M.; Bücher, C.; Hildebrand, G.; Schröter, B.; Weber, C.; Kempe, K.; Gottschaldt, M.; Liefeith, K.; Schubert, U. S. Amine End-Functionalized Poly(2-Ethyl-2-Oxazoline) as Promising Coating Material for Antifouling Applications. *J. Mater. Chem. B* **2014**, *2*, 4883−4893.
(26) Meldal, M.; Tornøe, C. W. Cu-Catalyzed Azide−Alkyne Cycloaddition. *Chem. Rev.* **2008**, *108*, 2952−3015.
(27) Rampal, J. B. *Microarrays*; Springer, 2007; Vol. *1*.
(28) Tu, Y.; Stolovitzky, G.; Klein, U. Quantitative Noise Analysis for Gene Expression Microarray Experiments. *Proc. Natl. Acad. Sci. U.S.A.* **2002**, *99*, 14031−14036.
(29) Hettegger, P.; Huber, J.; Paßecker, K.; Soldo, R.; Kegler, U.; Nöhammer, C.; Weinhäusel, A. High Similarity of IgG Antibody

Profiles in Blood and Saliva Opens Opportunities for Saliva Based Serology. *PLoS One* **2019**, *14*, No. e0218456.
(30) Bauch, M.; Toma, K.; Toma, M.; Zhang, Q.; Dostalek, J. Plasmon-Enhanced Fluorescence Biosensors: A Review. *Plasmonics* **2014**, *9*, 781−799.
(31) Vagias, A.; Sergelen, K.; Koynov, K.; Košovan, P.; Dostalek, J.; Jonas, U.; Knoll, W.; Fytas, G. Diffusion and Permeation of Labeled IgG in Grafted Hydrogels. *Macromolecules* **2017**, *50*, 4770.
(32) Laub, R.; Baurin, S.; Timmerman, D.; Branckaert, T.; Strengers, P. Specific Protein Content of Pools of Plasma for Fractionation from Different Sources: Impact of Frequency of Donations. *Vox Sang.* **2010**, *99*, 220−231.
(33) Fossati, S.; Hageneder, S.; Menad, S.; Maillart, E.; Dostalek, J. Multiresonant Plasmonic Nanostructure for Ultrasensitive Fluorescence Biosensing. *Nanophotonics* **2020**, *9*, 3673−3685.
(34) Baffou, G.; Quidant, R. Thermo-Plasmonics: Using Metallic Nanostructures as Nano-Sources of Heat. *Laser Photonics Rev.* **2013**, *7*, 171−187.

https://doi.org/10.1021/acsami.1c05950
ACS Appl. Mater. Interfaces 2021, 13, 27645−27655